Hindawi
BioMed Research International
Volume 2023, Article ID 9466110, 9 pages
https://doi.org/10.1155/2023/9466110

Research Article

Effect of Alleviating Fibrosis with EGCG-Modified Bone Graft in Murine Model Depended on Less Accumulation of Inflammatory Macrophage

Dengbo Yao, Jiang Guo, Tianyu Qin, Haibao Chen, and Song Jin

Department of Orthopedics Surgery, The Eighth Affiliated Hospital of Sun Yat-sen University, Shenzhen, China

Correspondence should be addressed to Song Jin; jingso@163.com

Received 31 March 2022; Revised 8 November 2022; Accepted 18 January 2023; Published 11 February 2023

Academic Editor: Cleofe Palocci

In response to current trends in the modification of guided bone regeneration (GBR) materials, we aimed to build upon our previous studies on epigallocatechin-3-gallate (EGCG) by immersing a commonly used bone graft primarily composed of hydroxyapatite (HA) in EGCG solution, expecting to obtain superior bone material integration after implantation. Bone grafts are commonly used for bone repair, in which the bone extracellular matrix is stimulated to promote osteogenesis. However, due to its profibrosis effect, this osteoconductive material commonly exhibits implant failure. In addition to providing a basic release profile of EGCG-modified bone graft (E-HA) to clarify the relationship between this material and the environment, we have examined the integration effect via subcutaneous implantation experiments. In this manner, we have assessed the aggregation of proinflammatory macrophages, the formation of fibrous capsules, and an enhanced cell viability observed in cultured RAW 264.7 cells. Among these results, we focus on proinflammatory macrophages due to their close relationship with fibrosis, which is the most important process in the immune response. Immunofluorescent staining results showed that E-HA substantially compromised the formation of fibrous capsules in hematoxylin-eosin-stained sections, which exhibited less proinflammatory macrophage recruitment; meanwhile, the cell viability was improved. This work lays the foundation for future studies on GBR.

1. Introduction

In guided bone regeneration (GBR), it is important to prevent the damaged area from being filled with soft tissue, leaving no space for bone tissue deposition. This aim can be attained by removing nonosteogenic tissues that interfere with bone regeneration while implanting biomaterials. The design of implanted bone substitutes should be based on the characteristics of the defect; moreover, these substitutes should restore the tissue microenvironment to its preimpairment state and avoid severe fibrosis to promote integration and function recovery [1, 2]. As a primary component of mineral bone, hydroxyapatite (HA), which constitutes 60%–70% of bone and 98% of dental enamel, exhibits good biocompatibility, high osteoconductivity [3], and a slow absorption rate at the implant site [4]. Accordingly, HA is one of the most widely used bone materials in clinical practice. In a 20-year follow-up study of maxillary sinus floor elevation based on commercial bovine-derived bone mineral, which is primarily composed of HA, the new mineralized bone volume remained stable and even increased from 16.96% to 22.05% over 20 years, while the volume of the implanted graft decreased from 35.87% to approximately 4% [5]. However, in some cases, HA implantation has resulted in disappointing or unsuccessful healing outcomes with thick fibrous capsules, which can inhibit bone–biomaterial integration via fibrosis. In addition, the formation of fibrous capsules is closely related to the host immune response, which has informed the design of next-generation GBR membranes and filling grafts based on a modulated immune microenvironment. With respect to biocompatibility, degradation rate, and mechanical support, the current mainstream clinical needs are no longer being met [6, 7]. Epigallocatechin-3-gallate (EGCG), the main catechin

of tea, has been considered a useful substance for modifying HA, due to its multiple therapeutic effects on various human diseases via its anti-inflammatory [8], anticarcinogenic [9], antimicrobial, and antioxidative ability [9]. In addition, in the field of bone remodeling, EGCG can promote osteogenesis with increased expression of bone morphogenetic protein-2 (BMP-2), runt-related transcription factor-2 (Runx-2), alkaline phosphatase (ALP), osteonectin, and osteocalcin. Thus, superior ALP activity and bone defect mineralization of bone defect can be achieved [10] to prevent inflammatory bone loss caused by inhibited prostaglandin E synthesis [11]. In a previous study, we found that the addition of EGCG to a designed material introduced a promising microenvironment for bone regeneration, based on macrophage recruitment and phenotype [12]. In macrophages, the persistence of inflammatory phenotypes can contribute to fibrosis, which impacts overall bone growth. Although the mechanism of fibrosis that occurs in implant biodegradation and the blocking interaction between the biomaterial and surrounding tissue requires further study, it has been confirmed that fibrosis is associated with the participation of certain macrophage phenotypes and various immune cells. The fibrosis response usually begins with a severe foreign body reaction (FBR) as cells are damaged, necrotized, and stressed [13, 14]. Nevertheless, principal cells that promote tissue repair are no different from those leading to fibrous capsules, except for the persistence and drastic communication of inflammatory cells and myofibroblasts [15]. In fact, with different degrees of fibrosis, the outcome of implantation can be beneficial for repair and prognosis (with the deposited provisional extracellular matrix (ECM) providing a frame for angiogenesis) or harmful to the host (impairing the integration and resulting in failure) [16]. Hence, the ideal situation is to avoid serious FBR and to enable direct healing by controlling the infiltrated cells and their ability to modulate the immune response. In summary, immunoreactions play a vital role in the healing process and determine the final result. Considering the broad clinical application of HA, it is valuable to understand the immune response invoked by the involvement of EGCG, which can reduce the level of proinflammatory macrophages. The purpose of the present study was to evaluate whether binding EGCG to HA can mitigate FBR with less fibrosis, thus enhancing bone regeneration.

2. Materials and Methods

2.1. Materials. We purchased commercial Heal-All® Bone Repair Material from Zhenghai Biotechnology (Shandong, China), which contains primarily HA and collagen and maintains a three-dimensional porous structure. EGCG was obtained from Jiang Xi Lv Kang Natural Products (Jiang Xi, China). The solvents and chemicals used were all of analytical grade, with no further purification. To fabricate EGCG-modified HA for follow-up experiments, we dissolved EGCG in aseptic double-distilled water at a concentration of 0.64% (w/v). We then immersed HA in the EGCG mixture for 24 h at 4°C in the dark [12, 16]. EGCG-modified bone graft (E-HA) was then washed with PBS three times and preserved in the dark at 4°C before use. The experimental process was conducted in accordance with the preservation protocol recommended by the manufacturer to avoid the oxidation denaturation of EGCG in light and heat. The optical density (OD) value of the EGCG solution at 272 nm was obtained before and after immersion to ensure successful fabrication of E-HA.

2.2. In Vitro Release Profile of E-HA. E-HA was soaked in PBS in a 48-well plate at 37°C and 5% CO_2 and scanned by ultraviolet–visible spectrophotometry to obtain the release profile. The OD value at 272 nm was used to detect EGCG in solution. At 0 h, the instrument was calibrated to zero; subsequently, we measured the OD value of the media at 2, 6, 12, 24, 48, 96, 120, 144, and 216 h. The media (200 μL) was removed and replenished with fresh buffer (200 μL) for each measurement. The solution concentration and EGCG weight were determined from an OD value for a specific concentration by establishing a standard curve with different concentrations (7.8, 15.625, 31.25, 62.5, 125, 250, and 500 μg/mL); the vertical axis shows the absorbance value, and the horizontal axis shows the concentration of the EGCG solution. Linear regression analysis was performed using the weighted least-square method ($W = 1/C^2$).

2.3. Surface Morphology Observation. A scanning electron microscope (SEM, s-800, HITACHI, Tokyo, Japan) operating at 15 kV under magnification of ×200, ×600, and ×1200 and a digital camera (Canon EOS 6D Mark II) under magnification of ×5 were used to characterize the morphology of the materials. A typical image of each sample was captured.

2.4. Cell Viability. Murine RAW264.7 cells (RIKEN BioResource Center, Japan) were used for quantitative and qualitative cell viability assays. The cells were cultured in 48-well plates and seeded on untreated and EGCG-treated HA at 10^4 cells/well cultured in 1640 medium supplemented with 10% fetal bovine serum. Immediately and after 1, 3, 5, and 7 days of culture, the cell viability was evaluated using Cell Counting Kit-8 (CCK-8, Dojindo Laboratories, Kumamoto, Japan) according to the manufacturer's instructions. The OD value at 450 nm was measured by a microplate reader (Multiskan, Thermo, USA).

2.5. Establishment of an In Vivo Model. This experimental protocol was approved by the Institutional Review Board of West China Dental Hospital (No. WCHSIRB-D-2017-097). *In vivo* experiments were performed on 6- to 8-week-old C57 mice (Animal Experimental Center of Sichuan University) weighing approximately 37.5 g. Two parallel surgical sites were established on each mouse for pure HA and E-HA, respectively ($N \geq 3$). To minimize the bias caused by the surgical site, the materials were implanted in different arrangements.

2.6. Surgical Procedures. After being anesthetized with intraperitoneal injection 80 mg/kg ketamine and 16 mg/kg xylazine at a volume of 10 μL/g weight, the skin on the back of the mouse above the surgical area was shaved, and an aseptic

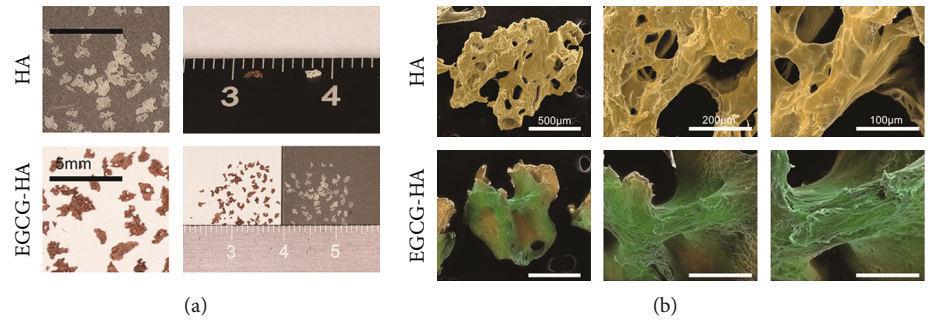

Figure 1: Representative image of HA and E-HA. (a) Surface morphology of materials is clearly presented under digital camera (magnification: ×5, bar = 5 mm) and (b) scanning electron microscope (magnification: ×200, ×600, ×1200, bar = 500 μm, 200 μm, 100 μm). The morphology is inconsistent in shape, size, and porous features between HA and E-HA. The surface of the bone repair material became less rough and more directional, dense, and uniform in E-HA.

process was applied before implantation. Two sagittal incisions of approximately 10 mm were made on the dorsal skin to create subcutaneous pockets for the bone repair material. Pure bone repair material and the EGCG-modified material were then implanted into the pockets. Subsequently, the incision was sutured with a horizontal mattress 3.0 Vicryl suture (Ethicon, CA, USA). The animals were housed in a room specially designed for animal experiments and were fed a standard laboratory diet. After 7 days of recovery, the animals were anesthetized by the above-mentioned anesthetic methods and then sacrificed by cervical dislocation. Then, the bone repair material and whole skin samples around the surgical site were collected. All experiments were performed according to the guidelines of animal ethics committee of Sichuan University.

2.7. Hematoxylin-Eosin (HE) Staining. For HE staining, 8 μm sections were incubated at 65°C for 4 h to dewax. After ethanol dehydration, hematoxylin was applied for 5 min, and 1% hydrochloric acid ethanol was differentiated for 2 h. The sections were then incubated for 2 min in 0.2% ammonia water, followed by staining with eosin for 1 min. After dehydration, the sections were removed and fixed with neutral resin. The slides were viewed using a microscope with a ×200 oil immersion objective (Olympus Corporation, Tokyo, Japan) and scanned with a digital slide scanning system (PRECICE, Beijing, China).

2.8. Immunofluorescent Staining. The paraffin-embedded tissue was cut into 8 μm-thick sections. After dewaxing and hydrating, immunostaining was conducted. Sections were pretreated with 0.1% Triton X-100 in PBS with 1% bovine serum albumin for 1 h, 1% t20 for 20 min, and then PBS for 20 min. Briefly, the sections were incubated for 30 min in the dark. The excess dye was washed away with PBS. Sections were incubated with isotype antibodies to exclude false positive staining. At least three parallel sections from different implantation sites were observed by fluorescence microscopy (Zeiss stereoscopic finding, V20, Germany). Five fields were randomly selected for immunofluorescence determination. Macrophages were magnified 400-fold to exclude false positive staining. Semiquantitative analysis was then performed at a magnification of 40-fold. CaseViewer 2.1 and Image Pro Plus 7.0 were used to measure the fluorescence intensity of five random spots. Hoechst (ab138903, Abcam) staining analysis was performed at the same time as CD68 (ab222914, Abcam) and inducible nitric oxide synthase (iNOS, ab209027, Abcam) analysis.

2.9. Statistical Analysis. All quantitative data are presented as the mean ± standard deviation. Statistical calculations were performed using GraphPad Prism 5.0 (San Diego, CA, USA). Semiquantitative immunofluorescent staining data that did not conform to the normal distribution were further analyzed by the Mann–Whitney U test, while the statistical significance between groups was analyzed by the analysis of variance, followed by Tukey's multiple-comparison test. A value of $P < 0.05$ was considered statistically significant. A standard curve for the EGCG solution was established by linear regression. Pearson's correlation analysis was used to analyze the detected concentration.

3. Results

3.1. Surface Morphology. The morphology of the bone repair material is shown in Figure 1(a). The morphology is inconsistent in shape, size, and porous features. After the addition of EGCG, the surface of the bone repair material became directional, dense, and uniform. This change may be caused by hydrogen bonding between the EGCG and collagen fibers. The SEM results also show that the surface roughness decreased (Figure 1(b)).

3.2. In Vitro Release Profile of E-HA. After HA was immersed in EGCG solution, the OD value decreased, indicating that the concentration had decreased and that E-HA had been successfully fabricated with EGCG adhering to the HA in the solution (Figure 2(a)). The calculated concentration was based on the standard curve for the EGCG solution. To establish this standard curve, EGCG solutions were detected by ultraviolet–visible spectrophotometry, which revealed that EGCG has a maximum absorption wavelength of 272 nm, regardless of the concentration. Therefore, 272 nm was selected for detection, and the absorbance value was set as the vertical axis with the corresponding concentration set as the horizontal axis. A regression equation

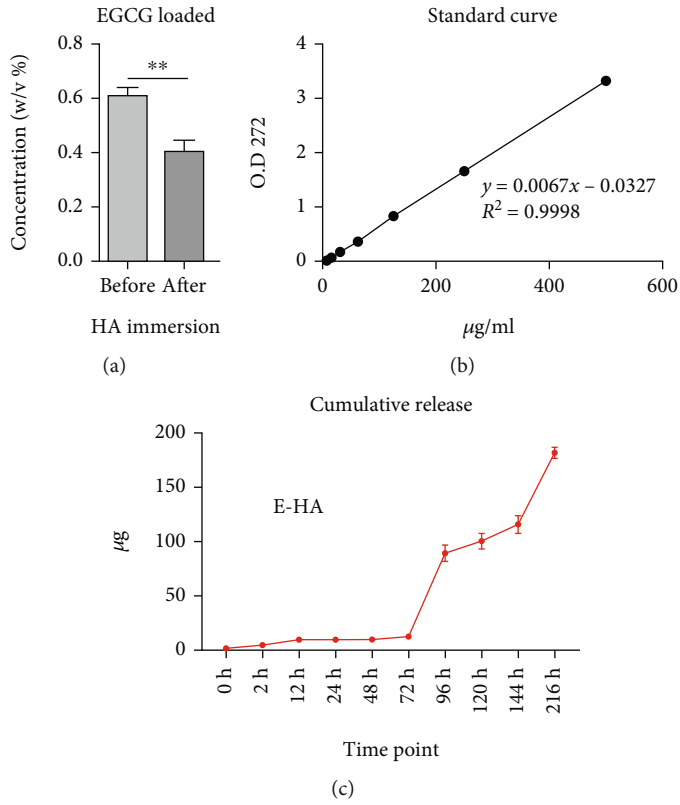

Figure 2: The establishment and release of EGCG on the bone graft. (a) E-HA fabrication assessment by detecting the concentration of EGCG solution before and after immersing HA ($n = 3$). (b) The standard curve of EGCG solution at the concentration between 7.8 and 500 μg/ml ($n = 3$), (c) obtained under OD value at 272 nm ($n = 3$). *In vitro* cumulative release profile of E-HA. ns: no significance; $^{*}P < 0.05$, $^{**}P < 0.01$, $^{***}P < 0.001$.

was obtained as $y = 0.0067x - 0.0327$, with $R^2 = 0.9998$. The linear concentration range was found to be 7.8–500 μg/mL for EGCG, as presented in Figure 2(b). A cumulative release profile of E-HA was obtained by detecting the amount of EGCG released to the buffer over time. With the obtained standard curve line, we can interpret the EGCG concentration corresponding to OD values measured at different time points in the cumulative release profile. The release profile demonstrated a minimal initial release, with only approximately 10 μg EGCG being released in the first 3 days, followed by a continuous release reaching approximately 100 μg over the next 3 days. An additional release of approximately 75 μg was measured at 216 h (Figure 2(c)).

3.3. Cell Viability. RAW 264.7 cells were seeded on the material for 7 days; throughout this period, the cell viability remained relatively constant for the HA group, whereas the effect of EGCG on cell viability increased as the coculture time increased. On days 0 and 1, there was no significant difference between the HA and E-HA groups; however, on days 3 and 5, the cell viability improved slightly in the group with EGCG. The viability continued to increase, reaching a maximum on day 7 (Figure 3). Thus, the modification of EGCG did not negatively impact cell viability in RAW 264.7 cells; rather, EGCG appears to improve cell viability.

3.4. Fibrosis Severity after HA and E-HA Implantation in Relation to Macrophage Phenotype. To determine whether E-HA can mitigate fibrosis by modulating the immune microenvironment, the selected materials were implanted subcutaneously (Figures 4(a) and 4(b)), and the reaction of immune cells towards EGCG modification was investigated by HE staining (Figures 4(c) and 4(d)). Within 7 days after implantation of the bone repair material, the incisions of both groups had healed well. The fibrous encapsulation effect was much more intense in the HA group, with a large amount of collagen fibers deposited on the surface of the material. The surrounding immune cells migrated to the bone repair material, forming an inflammatory cell infiltration zone. This inflammation resulted from the implantation of EGCG-loaded bone repair material, which is lighter than pure bone repair material. We further explored the macrophage phenotype at this time point. Based on Hoechst, CD68, and iNOS immunofluorescence staining images (Figures 4(e) and 4(f)), we found that the two groups recruited macrophages of different phenotypes. CD68, which serves as a surface marker for macrophages, was observed in both groups. However, iNOS, an indicator of proinflammatory phenotype macrophages, was not detected in the E-HA group, although it was detected in the HA group, reconfirming macrophage infiltration and the effect of EGCG on anti-inflammation, as shown in Figures 5(a) and 5(b).

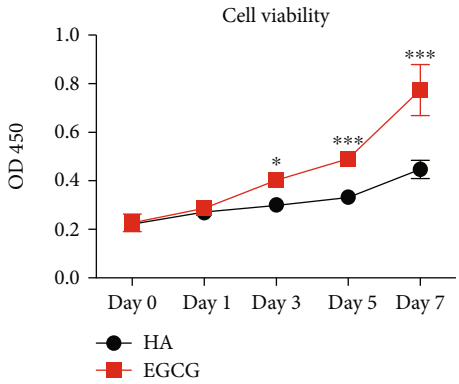

FIGURE 3: Cell viability assay. Culturing RAW 264.7 on deproteinized bone material with or without EGCG treatment; then optical density (OD) was detected at a wavelength of 450 nm on days 0, 1, 3, 5, and 7 to evaluate cell viability ($n = 3$). ns: no significance; $^{*}P < 0.05$, $^{**}P < 0.01$, $^{***}P < 0.001$.

4. Discussion

Serious defects in hard tissue can inhibit self-healing, with critical-sized bone defects requiring surgical intervention [17]. At the present, biomaterials and GBR membranes are often used in clinical practice to block the invasion of soft tissue in the growth space of the hard tissue, a practice that has been widely validated. Among these materials, collagen membranes modified by EGCG have been thoroughly investigated, including studies on their biotoxicity [18], effect on osteoblasts [19], chemotaxis of macrophages [20], phenotypic regulation [21], and FBR [22]. The ideal therapeutic effect of an implanted biomaterial cannot be achieved if the stimulating effect due to modification is neglected. For example, biomaterials often include HA, such as BMP-2-immobilized PLGA/hydroxyapatite fibrous scaffold [23], or have been modified, for example, by loading nerve growth factor [24], which can promote tissue repair better than the materials alone. When a biomaterial is implanted, material will interact with the immune cells to form a unique immune microenvironment, which is very crucial for the subsequent bone tissue healing process. Macrophages have been proven to effectively regulate the bone immune microenvironment [25]. After surgery, macrophages quickly identify the implant, are recruited to the biomaterial, and form a specific immune microenvironment. Studies have shown that proinflammatory macrophages known as M1 participate in the initiation of inflammation by secreting cytokines and then proinflammatory macrophages known as M2 participate in tissue remodeling. A transformation in the macrophage phenotype from proinflammatory to anti-inflammatory is necessary in both hard- and soft-tissue repair. As one of the primary causes of implant failure, aseptic loosening is caused by the formation of wear particles from the implant under phagocytosis, which promotes macrophage secretion of cytokines related to bone absorption [26]. HA-induced phagocytosis depends on IL-1β and TNF-α produced by macrophages [26], which are closely related to the proinflammatory phenotype. Furthermore, a long-term high proinflammatory/anti-inflammatory phenotypic ratio of macrophages often indicates implantation failure. Thus, in addition to manufacturing biomaterials similar to the natural ECM, the phenotype of macrophages should also be considered. A biodegradable three-dimensional scaffold comprising polymer matrix (polylactic acid and polyethylene glycol), nano-HA, and dexamethasone has been shown to promote macrophage polarization towards the anti-inflammatory phenotype and osteogenesis, in which proinflammatory macrophages downregulate IL-6 and iNOS expression [27]. In fact, both proinflammatory and anti-inflammatory phenotypes are indispensable for tissue healing, and proinflammatory macrophages can even guide the subsequent behavior of anti-inflammatory macrophages. Previous studies have shown that collagen membrane loaded with EGCG can induce M2 macrophages to polarize and increase osteogenic activity and promote bone healing [12]. Except for promoting osteogenesis, another important reason for graft failure is that the material is wrapped by fibrous tissue. We used EGCG-modified HA to investigate its effect on the phenotype of macrophages and its effect on fibrosis. As CD68 is widely acknowledged as a marker for macrophages, which is applied to identify the presence of macrophages, iNOS is a marker of M1 macrophages. In this study, we found that the addition of EGCG reduced the activation of M1 macrophages. Moreover, HE staining showed that E-HA significantly reduced the fibrotic encapsulation around the material, suggesting that the decrease of M1 macrophages was related to the inhibition of fibrosis. A recent study showed that reducing the activation of M1 macrophages and increasing the ratio of M2/M1 cells can help to reduce fibrosis, which is consistent with our results [28]. Another study showed that long-term or severe inflammation usually contributes to fibrous capsule formation by activating anti-inflammatory macrophages releasing fibrotic cytokines, which block the surrounding material and eventually lead to bone–biomaterial integration failure [29]. This conclusion is different from ours, which may be due to the fact that EGCG suppresses inflammation at the beginning, thus alleviating the effect of M2 on fibrosis in the later stage of repair, because successful repair can never be accompanied by excessive proinflammatory polarization [30]. In fact, both proinflammatory and anti-inflammatory phenotypes are indispensable for tissue healing, and proinflammatory macrophages can even guide the subsequent behavior of anti-inflammatory macrophages. Apart from inhibiting proinflammatory macrophages, we also found that EGCG altered its surface morphology of HA by scanning electron microscope, and its surface morphology became denser and less rough. A previous study showed that the polarization of macrophages is regulated by the surface morphology of materials, and the increase of surface roughness can induce the polarization of anti-inflammatory macrophages, on the contrary, the finer surface morphology is more inclined to M1 polarization [31]. However, our study found that E-HA inhibited the activation of M1, which may be related to the anti-inflammatory and the polarization of M2 macrophages induced by EGCG [8, 10]. Cytotoxicity is another essential aspect to evaluate when considering

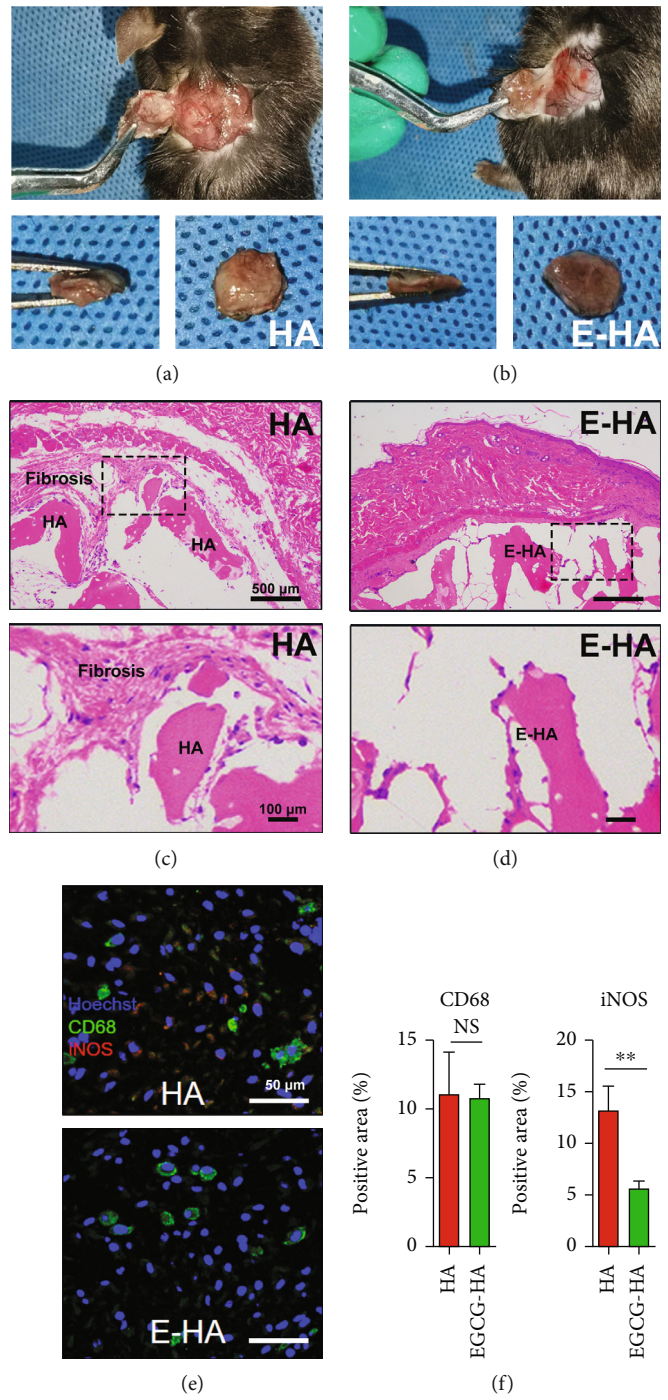

Figure 4: Evaluation of fibrosis and phenotype of infiltrating macrophages after implantation. Pictures of harvested tissue: (a) HA and (b) E-HA. (c, d) HE staining result ($n = 3$) on day 7 postsurgery (upper panel, bar = 500 μm; lower panel, bar = 100 μm). (e) Immunofluorescent staining result on day 7 postsurgery ($n = 3$). Hoechst, blue; CD68, green; iNOS, red (bar = 50 μm). (f) Semiquantitative analysis of immunofluorescent staining result ($n = 3$). ns: no significance; $^{*}P < 0.05$, $^{**}P < 0.01$, $^{***}P < 0.001$.

biocompatibility. However, further investigation is needed to determine whether EGCG can promote the polarization of macrophages towards anti-inflammatory phenotypes and stimulate the secretion of desired cytokines. Our results showed cell viability was improved by the addition of EGCG. We found that the effect of EGCG on cell viability was related to its release from E-HA. Our *in vitro* EGCG release rate assay showed that more EGCG was released over time. As the culture time increased, the effect of EGCG on cell viability grew. Therefore, it is suggested that the addition of EGCG will not reduce, and may even increase, cell activity, which ensures good cellular function and subsequent tissue healing. In this article, we only focused on the study of E-HA reducing proinflammatory macrophages and reducing

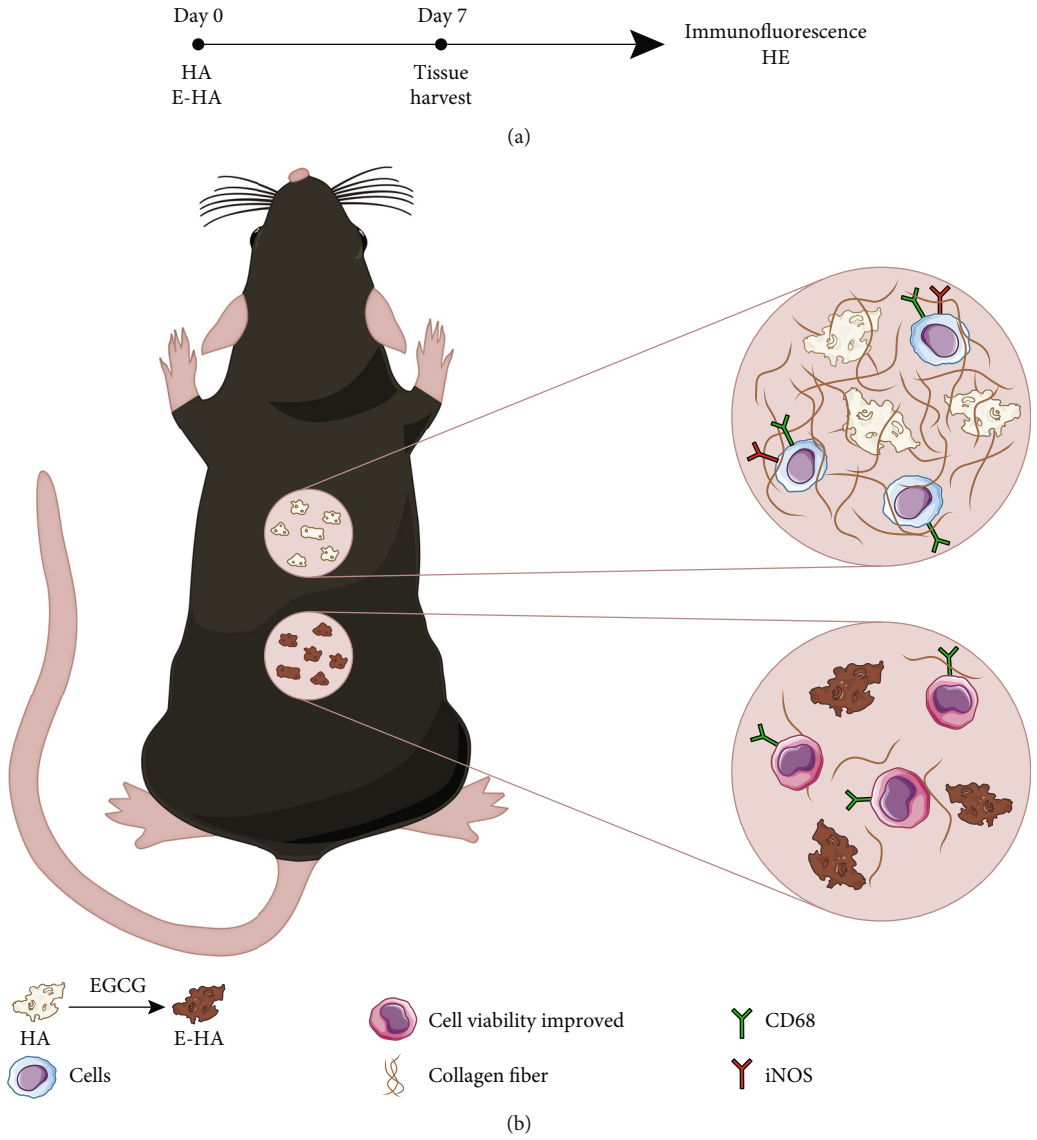

Figure 5: Schematic illustration. Diagram of *in vivo* experiments. (a) Showing the period to harvest and the subsequently executed testing. (b) Cell viability, macrophage polarization, and fibrosis outcome of EGCG-modified bone graft, compared with bone graft alone.

fibrosis in subcutaneous models. However, further studies are needed to determine whether E-HA can promote the polarization of macrophages to anti-inflammatory phenotypes and stimulate the secretion of required cytokines to promote osteogenesis, as well as the ratio of proinflammatory/anti-inflammatory macrophages at different time points, which will be discussed in future bone models.

5. Conclusion

In summary, we have presented a potential strategy for modifying bone repair material. This strategy provides an anti-inflammatory effect by reducing the accumulation of proinflammatory macrophages and further regulates fibrosis, although the effect of EGCG on the surface morphology cannot be excluded. The specific mechanism leading to reduced fibrosis requires verification. The results of this study will pave the way for subsequent experiments and for further work on the osteogenesis effect of E-HA, as this is an essential effect of bone repair materials. Under the studied circumstances, the addition of EGCG to HA improved cell activity, and no $CD68^{+}iNOS^{+}$ cells were detected by immunofluorescence staining at 7 days postsurgery, indicating that the addition of EGCG may resolve the following regenerative cascade. The contents in the article are quoted from the preprint [32].

Data Availability

The data supporting the findings of this study are available from the corresponding author on reasonable request.

Disclosure

This article has been presented as a preprint according to the following link https://www.biorxiv.org/content/10.1101/2020.11.10.376590v4.

Conflicts of Interest

There are no conflicts of interest related to this manuscript.

Authors' Contributions

Dengbo Yao and Jiang Guo contributed equally to this work.

Acknowledgments

This work was supported by the Shenzhen Key Medical Discipline Construction Fund (SZXK086). And special thanks are due to Dr. Shengan Rung's assistance.

References

[1] K. L. Christman, "Biomaterials for tissue repair," *Science*, vol. 363, no. 6425, pp. 340-341, 2019.

[2] K. Sadtler, A. Singh, M. T. Wolf, X. Wang, D. M. Pardoll, and J. H. Elisseeff, "Design, clinical translation and immunological response of biomaterials in regenerative medicine," *Nature Reviews Materials*, vol. 1, no. 7, p. 16040, 2016.

[3] S. R. Dutta, D. Passi, P. Singh, and A. Bhuibhar, "Ceramic and non-ceramic hydroxyapatite as a bone graft material: a brief review," *Irish Journal of Medical Science*, vol. 184, no. 1, pp. 101–106, 2015.

[4] J. T. B. Ratnayake, M. Mucalo, and G. J. Dias, "Substituted hydroxyapatites for bone regeneration: a review of current trends," *Journal of Biomedical Materials Research. Part B, Applied Biomaterials*, vol. 105, no. 5, pp. 1285–1299, 2017.

[5] P. Valentini and D. D. Bosshardt, "20-year follow-up in maxillary sinus floor elevation using bovine-derived bone mineral: a case report with histologic and histomorphometric evaluation," *The International Journal of Oral & Maxillofacial Implants*, vol. 33, no. 6, pp. 1345–1350, 2018.

[6] H. S. Joo, J. H. Suh, H. J. Lee, E. S. Bang, and J. M. Lee, "Current knowledge and future perspectives on mesenchymal stem cell-derived exosomes as a new therapeutic agent," *International Journal of Molecular Sciences*, vol. 21, no. 3, p. 727, 2020.

[7] I. Rodriguez, S. Gs, A. Fetz et al., "Barrier membranes for dental applications: a review and sweet advancement in membrane developments," *Mouth and Teeth*, vol. 2, 2018.

[8] T. Ohishi, S. Goto, P. Monira, M. Isemura, and Y. Nakamura, "Anti-inflammatory action of green tea," *Anti-Inflammatory & Anti-Allergy Agents in Medicinal Chemistry*, vol. 15, no. 2, pp. 74–90, 2016.

[9] A. Negri, V. Naponelli, F. Rizzi, and S. Bettuzzi, "Molecular targets of epigallocatechin-Gallate (EGCG): a special focus on signal transduction and cancer," *Nutrients*, vol. 10, no. 12, p. 1936, 2018.

[10] S. Y. Lin, L. Kang, C. Z. Wang et al., "(-)-Epigallocatechin-3-gallate (EGCG) enhances osteogenic differentiation of human bone marrow mesenchymal stem cells," *Molecules*, vol. 23, no. 12, p. 3221, 2018.

[11] T. Tominari, R. Ichimaru, S. Yoshinouchi et al., "Effects of O-methylated (−)-epigallocatechin gallate (EGCG) on LPS-induced osteoclastogenesis, bone resorption, and alveolar bone loss in mice," *FEBS Open Bio*, vol. 7, no. 12, pp. 1972–1981, 2017.

[12] C. Chu, Y. Wang, Y. Wang et al., "Evaluation of epigallocatechin-3-gallate (EGCG) modified collagen in guided bone regeneration (GBR) surgery and modulation of macrophage phenotype," *Materials Science & Engineering. C, Materials for Biological Applications*, vol. 99, pp. 73–82, 2019.

[13] B. A. Shook, R. R. Wasko, G. C. Rivera-Gonzalez et al., "Myofibroblast proliferation and heterogeneity are supported by macrophages during skin repair," *Science*, vol. 362, no. 6417, 2018.

[14] R. Klopfleisch and F. Jung, "The pathology of the foreign body reaction against biomaterials," *Journal of Biomedical Materials Research. Part A*, vol. 105, no. 3, pp. 927–940, 2017.

[15] P. Pakshir and B. Hinz, "The big five in fibrosis: macrophages, myofibroblasts, matrix, mechanics, and miscommunication," *Matrix Biology*, vol. 68-69, pp. 81–93, 2018.

[16] L. Tang and J. W. Eaton, "Inflammatory responses to biomaterials," *American Journal of Clinical Pathology*, vol. 103, no. 4, pp. 466–471, 1995.

[17] A. Nauth, E. Schemitsch, B. Norris, Z. Nollin, and J. T. Watson, "Critical-size bone defects: is there a consensus for diagnosis and treatment?," *Journal of Orthopaedic Trauma*, vol. 32, no. 3, pp. S7–s11, 2018.

[18] C. Chu, J. Deng, Y. Hou et al., "Application of PEG and EGCG modified collagen-base membrane to promote osteoblasts proliferation," *Materials Science & Engineering. C, Materials for Biological Applications*, vol. 76, pp. 31–36, 2017.

[19] C. Chu, J. Deng, L. Xiang et al., "Evaluation of epigallocatechin-3-gallate (EGCG) cross-linked collagen membranes and concerns on osteoblasts," *Materials Science & Engineering. C, Materials for Biological Applications*, vol. 67, pp. 386–394, 2016.

[20] X. Hua, S. Ge, M. Zhang et al., "Pathogenic roles of CXCL10 in experimental autoimmune prostatitis by modulating macrophage chemotaxis and cytokine secretion," *Frontiers in Immunology*, vol. 12, article 706027, 2021.

[21] S. A. Almatroodi, A. Almatroudi, M. A. Alsahli, M. A. Aljasir, M. A. Syed, and A. H. Rahmani, "Epigallocatechin-3-gallate (EGCG), an active compound of green tea attenuates acute lung injury regulating macrophage polarization and Krüppel-like-factor 4 (KLF4) expression," *Molecules*, vol. 25, no. 12, p. 2853, 2020.

[22] C. Chu, L. Liu, Y. Wang et al., "Macrophage phenotype in the epigallocatechin-3-gallate (EGCG)-modified collagen determines foreign body reaction," *Journal of Tissue Engineering and Regenerative Medicine*, vol. 12, no. 6, pp. 1499–1507, 2018.

[23] X. Zhao, Y. Han, J. Li et al., "BMP-2 immobilized PLGA/hydroxyapatite fibrous scaffold via polydopamine stimulates osteoblast growth," *Materials Science & Engineering. C, Materials for Biological Applications*, vol. 78, pp. 658–666, 2017.

[24] X. Han, H. Liu, X. Kuang, Z. Wang, and X. Wang, "Silk fibroin improves the release of nerve growth factor from hydroxyapatite particles maintaining its bioactivity," *Current Drug Delivery*, vol. 15, no. 6, pp. 879–886, 2018.

[25] J. Ping, C. Zhou, Y. Dong et al., "Modulating immune microenvironment during bone repair using biomaterials: focusing on the role of macrophages," *Molecular Immunology*, vol. 138, pp. 110–120, 2021.

[26] V. K. Gopinath, M. Musa, A. R. Samsudin, and W. Sosroseno, "Role of interleukin-1beta and tumour necrosis factor-alpha on hydroxyapatite-induced phagocytosis by murine macrophages (RAW264.7 cells)," *British Journal of Biomedical Science*, vol. 63, no. 4, pp. 176–178, 2006.

[27] Q. L. Ma, L. Z. Zhao, R. R. Liu et al., "Improved implant osseointegration of a nanostructured titanium surface via

mediation of macrophage polarization," *Biomaterials*, vol. 35, no. 37, pp. 9853–9867, 2014.

[28] K. E. Martin and A. J. García, "Macrophage phenotypes in tissue repair and the foreign body response: implications for biomaterial-based regenerative medicine strategies," *Acta Biomaterialia*, vol. 133, pp. 4–16, 2021.

[29] H. Fang, C. Luo, S. Liu et al., "A biocompatible vascularized graphene oxide (GO)-collagen chamber with osteoinductive and anti-fibrosis effects promotes bone regeneration in vivo," *Theranostics*, vol. 10, no. 6, pp. 2759–2772, 2020.

[30] C. Chu, L. Liu, S. Rung et al., "Modulation of foreign body reaction and macrophage phenotypes concerning microenvironment," *Journal of Biomedical Materials Research. Part A*, vol. 108, no. 1, pp. 127–135, 2020.

[31] K. M. Hotchkiss, G. B. Reddy, S. L. Hyzy, Z. Schwartz, B. D. Boyan, and R. Olivares-Navarrete, "Titanium surface characteristics, including topography and wettability, alter macrophage activation," *Acta Biomaterialia*, vol. 31, pp. 425–434, 2016.

[32] D. Yao and S. Jin, "Effect of alleviating fibrosis with EGCG-modified bone graft in murine model depended on less accumulation of inflammatory macrophage," *bioRxiv*, 2022.